

Application of Hexanoyl Glycol Chitosan as a Non-cell Adhesive Polymer in Three-Dimensional Cell Culture

Da-Eun Kim,[#] Yu Bin Lee,[#] Hye-Eun Shim, Jin Jung Song, Ji-Seok Han, Kyoung-Sik Moon, Kang Moo Huh,^{*} and Sun-Woong Kang^{*}



Cite This: *ACS Omega* 2022, 7, 18471–18480



Read Online

ACCESS |



Metrics & More

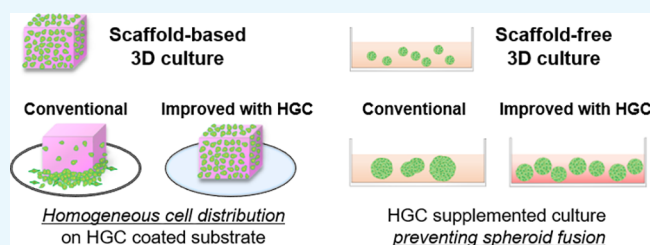


Article Recommendations



Supporting Information

ABSTRACT: Cell culture technology has evolved into three-dimensional (3D) artificial tissue models for better reproduction of human native tissues. However, there are some unresolved limitations that arise due to the adhesive properties of cells. In this study, we developed a hexanoyl glycol chitosan (HGC) as a non-cell adhesive polymer for scaffold-based and -free 3D culture. The uniform cell distribution in a porous scaffold was well maintained during the long culture period on the HGC-coated substrate by preventing ectopic adhesion and migration of cells on the substrate. In addition, when culturing many spheroids in one dish, supplementation of the culture medium with HGC prevented the aggregation of spheroids and maintained the shape and size of spheroids for a long culture duration. Collectively, the use of HGC in 3D culture systems is expected to contribute greatly to creating excellent regenerative therapeutics and screening models of bioproducts.



INTRODUCTION

Cell culture technology serves as a central tool in the fields of biotechnology and regenerative medicine.¹ Two-dimensional (2D) cell culturing was first performed using flat polystyrene Petri plates. Until recently, this method was considered the gold standard because of its convenience and high reproducibility. With advances in technology, three-dimensional (3D) cell culture methods were developed for extensive evaluation.² Beyond the treatment of damaged tissue, models of 3D cell culture technology with controlled variables have emerged to study unknown biological phenomena and evaluate bioproducts.³ However, despite its various advantages, the technology has demonstrated limitations in its use due to the complexity of culture and low reproducibility.

Typical 3D culture is divided into two methods, scaffold-based systems involving culturing of cells on pre-configured 3D scaffolds and scaffold-free systems that form spheroids.⁴ The adhesive property of cells is a key prerequisite for both systems. Cell adhesion on natural and/or synthetic polymers allows the development of scaffold-based 3D constructs. In addition, cells on ultralow attachment (ULA) dishes compose spheroids by adhering to each other.⁵ Although the adhesive property of cells plays a pivotal role in the formation of a 3D structure, it may interfere with the maintenance of the shape and function of 3D constructs during long-term culture. For instance, after seeding cells into the scaffold, they are cultured on flat plates, such as Petri dishes, for tissue regeneration.⁶ Consequently, the cells in the 3D constructs spread and proliferate ectopically on the surface of the dish because of the adhesive property of cells

while regenerating the tissue in the scaffold.⁷ Even in a spheroid culture, the spheroids randomly aggregate with each other due to the forces of cell attachment. This phenomenon reduces the homogeneity of the size and the biological function of spheroids.^{8,9} In this regard, developing an appropriate environment that can overcome these limitations is critical to ensure reproducibility and cellular function during the culture of 3D constructs.

Accumulating evidence has shown that the ULA surface can be designed for maintaining cells in a suspended form, reducing attachment of anchorage-dependent cells to the substrate, and formation of 3D multicellular spheroids.¹⁰ Chitosan has been successfully used as an ultralow cell adhesive material. A chitosan-coated surface inhibits the attachment of cells and facilitates spheroid formation.¹¹ However, chitosan alone is insufficient for the non-adhesive property. Therefore, numerous studies have focused on the chemical modification of amino and hydroxyl groups in the main molecular structure of chitosan. Particularly, *N*-hexanoyl glycol chitosan (HGC), a type of *N*-acylated glycol chitosans (NAGCs), is easily soluble under neutral pH and enables the efficient formation of 3D cell spheroids due to non-adhesive

Received: February 13, 2022

Accepted: May 16, 2022

Published: May 26, 2022



properties.¹² However, these studies to date have not addressed the effect on the behavior of cells in scaffolds and the spheroid–spheroid fusion. No studies have demonstrated non-cell adhesive materials for uniform cell distribution into scaffold and prevention of spheroid fusion during 3D cell culture. We hypothesized that usage of HGC in 3D cell culture overcomes the aforementioned limitations by preventing ectopic cell attachment from the scaffold and spheroid fusion due to the non-cell adhesive property. To that end, in this study, we examined the effect of HGC on both scaffold-based and scaffold-free cell cultures to suggest a new 3D cell culture strategy (Figure 1). We evaluated whether HGC-coated dishes

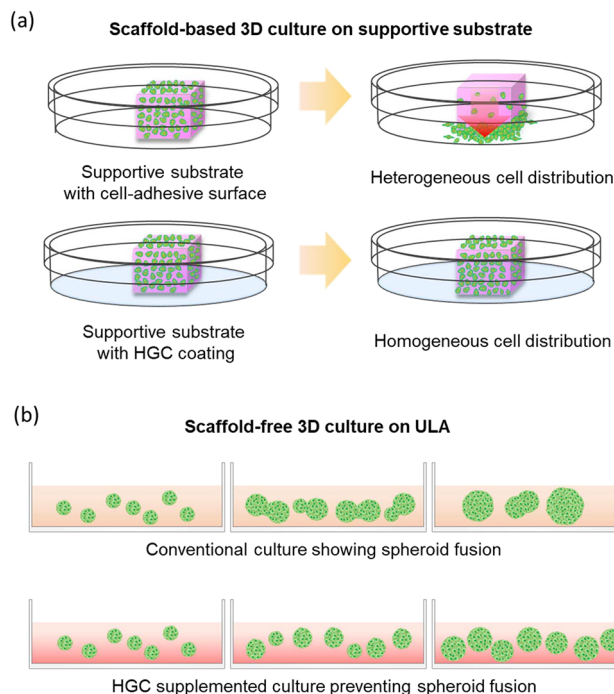


Figure 1. Schematic illustration of conventional 3D cultures and improvements hypothesized by introduction of hexanoyl glycol chitosan (HGC). (a) Culture of scaffold-based 3D constructs on supportive substrates with cell-adhesive or HGC-coated surfaces. (b) Schematic illustration of scaffold-free spheroid culture on conventional ultralow attachment dishes with or without HGC supplementation.

affected the maintenance of uniform cell distribution within the cell seeded 3D scaffold constructs. Next, it was evaluated whether spheroid fusion was prevented when many spheroids were cultured in one dish by the effect of supplemented HGC in the cell culture medium. Collectively, we aimed to improve both scaffold-based and scaffold-free 3D tissue culture systems by exploiting the properties of HGC.

MATERIALS AND METHODS

Materials. Glycol chitosan (GC, DP \geq 200) was purchased from WAKO Pure Chemical Industries, Ltd. (Osaka, Japan). Hexanoic anhydride (97%) was purchased from Sigma-Aldrich (MA, USA). Acetone and methanol were supplied by Samchun Chemical (Pyeongtaek, Korea). A dialysis membrane (12–14 kDa) was supplied by Spectrum Laboratories (CA, USA). Cell Counting Kit-8 (CCK-8) was purchased from Dojindo Laboratories (Kumamoto, Japan). Collacote (collagen sponge) was purchased from Zimmer Biomet (IN, USA). A LIVE/

DEAD Viability/Cytotoxicity Kit for mammalian cells was purchased from Invitrogen. The Wizard Genomic DNA Purification Kit was purchased from Promega (WI, USA).

Synthesis of HGC. HGC was synthesized via *N*-hexanoylation of GC. Briefly, 3 g of GC was dissolved in 375 mL of distilled water followed by the addition of 375 mL of methanol. Hexanoic anhydride (1.119 mL) was added to the GC solution with vigorous stirring at RT. The reacted polymer was purified via precipitation in an excess amount of acetone. The precipitate of HGC was dissolved in distilled water and then dialyzed for 2 days (molecular weight cutoff 12 kDa). The purified solution was obtained in powder form via freeze-drying. GC and HGC were characterized via ¹H-NMR spectroscopy with an AVANCE III 600 spectrometer (Bruker, Bremen, Germany) at 600 MHz. The polymers were dissolved in D₂O at a concentration of 1.0 wt %. The attenuated total reflectance Fourier transform infrared (ATR-FTIR) spectra of GC and HGC were recorded using a Nicolet iS5 spectrometer (Thermo Scientific, MA, USA). The analysis was performed with 16 scans obtained at a resolution of 4 cm⁻¹ over a frequency range of 4000–660 cm⁻¹.

Cell Culture. HepG2 cells (ATCC, VA, USA) were cultured and maintained in MEM containing 10% fetal bovine serum and 1% P/S (growth media) on regular tissue culture plates (TCP). Cell culture was performed under standard conditions (95% humidity, 5% CO₂, 37 °C). Chondrocytes were isolated from 4-week-old New Zealand white rabbits (Orient, Sungnam, Korea) by articular cartilage biopsy. Briefly, the articular cartilage was minced and digested with 0.05 w/v % type II collagenase solution (Sigma Aldrich, MA, USA).¹³ The isolated cells were washed thrice with PBS and cultured with DMEM. The medium was replaced every 2 days. Cells were collected from TCP for passage and experiments via a regular trypsinization procedure (0.05% trypsin/EDTA).

All animal studies for isolation of chondrocytes were performed in compliance with the guidelines of the Institutional Animal Care and Use Committee (IACUC 1304-0113) of the Korea Institute of Toxicology (KIT) and the guidelines for the care and use of laboratory animals of the National Research Council. All experiments were approved by the animal ethics committee of KIT.

Cytotoxicity Test of HGC. The cytotoxicity of HGC was estimated using CCK-8. HepG2 cells were plated in 96-well tissue culture plates (Corning Costar, NY, USA) at a density of 1×10^3 cells/well in MEM containing 10% fetal bovine serum and 1% P/S and incubated for 1 day. After 24 h of incubation, the culture medium was replaced with MEM containing various concentrations of HGC (0, 0.25, 0.5, and 1 wt %). After 0, 1, 3, 5, and 7 days of culture in the medium with different concentrations of HGC, 10 μ L of CCK solution was directly added to each well, and the samples were incubated at 37 °C for 2 h. An intense orange-colored and water-soluble formazan derivative was formed via cellular metabolism in the culture medium. The OD value for the culture medium was analyzed at a wavelength of 450 nm using a microplate reader (VersaMax, Molecular Devices, CA, USA). The relative proliferation rate was calculated by normalizing data observed at each time point with data recorded at day 0.

Preparation of HGC-Coated Petri Dish. HGC (0.5 wt %) was dissolved in autoclaved and filtered distilled water and maintained at 4 °C. The polymer solution (0.9 mL) was added to each 60 mm Petri dish (SPL Life Sciences Co., Ltd., Seoul,

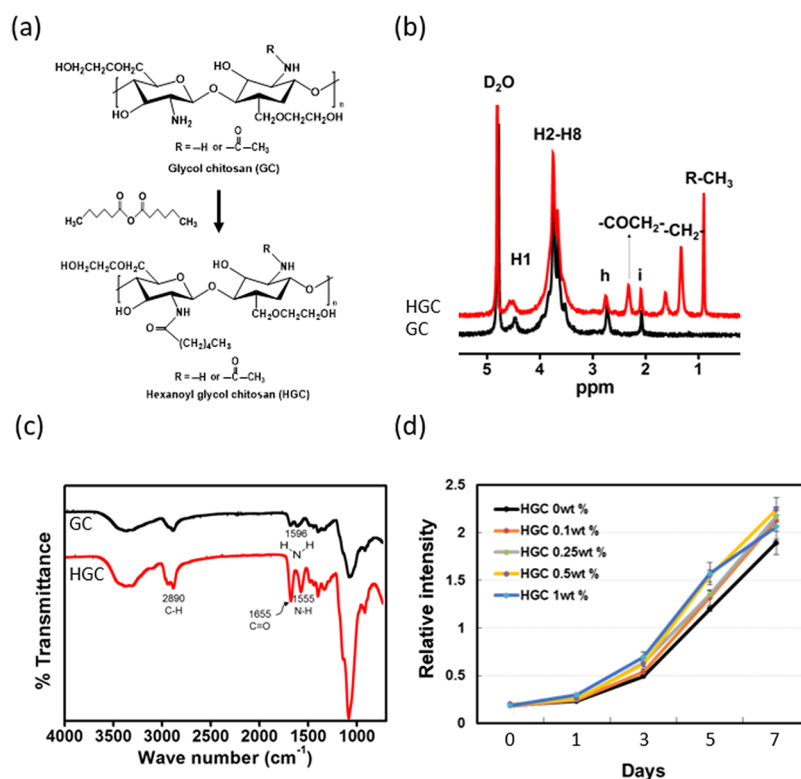


Figure 2. (a) Synthetic procedure for HGC. (b) $^1\text{H-NMR}$ spectra of glycol chitosan (GC) (black) and HGC (red). (c) ATR-FTIR spectra of GC (black) and HGC (red). (d) *In vitro* cytotoxicity study of HGC against HepG2 cells.

Korea) and spread. The solution was then dried at $55\text{ }^\circ\text{C}$ overnight to obtain an HGC-coated Petri dish.

Preparation and Culture of Scaffold-Based 3D Constructs. Collagen sponges ($2 \times 5.0 \times 3.0\text{ mm}^3$) were immersed in growth media with FBS (10%) for 24 h before cell seeding. HepG2 cells and chondrocyte suspension in the growth media ($20\text{ }\mu\text{L}$, 2.5×10^6 cells/mL) were seeded into the collagen sponge. The constructs were incubated in the growth media on Petri dishes at $37\text{ }^\circ\text{C}$ for 24 h. Next, the constructs of HepG2 cells and chondrocytes were transferred to the Petri dishes, cell culture dishes, and HGC-coated dishes and then cultured for 2 and 4 weeks, respectively.

Live/Dead Assay. Cell viability was determined via LIVE/DEAD Viability/Cytotoxicity Kit for mammalian cells (Invitrogen, CA, USA). Prepared samples were treated with 0.1% calcein AM and 0.2% ethidium homodimer-1 in PBS for 15 min at $37\text{ }^\circ\text{C}$ and subsequently examined via confocal laser-scanning microscopy (LSM 800, Carl Zeiss, Oberkochen, Germany) under optimized observation conditions of Calcein AM (EX-495 nm/EM-515 nm) and ethidium homodimer-1 (EX-528 nm/EM-617 nm).

Proliferation of Cells in Scaffold-Based 3D Constructs. Cell proliferation was evaluated using CCK-8. At designated time points, the HepG2 cell-seeded collagen sponges were incubated in CCK-8 solution at $37\text{ }^\circ\text{C}$ for 3 h. Intense orange-colored formazan derivatives formed via cellular metabolism were soluble in the culture medium. The absorbance of the supernatants of the samples was measured at 450 nm. An ATP assay was performed for luminometric measurement of cell growth (viability) according to the standard protocol of the manufacturer (CellTiter-Glo 3D Cell Viability Assay, Promega, WI, USA). Multiwell plates with opaque walls were prepared with microtissues in a culture

medium. The plates were equilibrated, and their contents were incubated at RT for approximately 30 min. Next, $100\text{ }\mu\text{L}$ of a reagent was added to an equal volume of cell culture medium present in each well. The plates were incubated at RT for an additional 25 min to stabilize the luminescence signals followed by the measurement of luminescence using a microplate reader (VersaMax, Molecular Devices, CA, USA) ($n = 6$).

Histology of Scaffold-Based 3D Constructs and Assessment of Cellular Distribution. Samples cultured on uncoated Petri dishes, cell culture dishes, and HGC-coated dishes were collected and fixed with 2.5% glutaraldehyde at different intervals. The fixed samples were embedded in paraffin and divided into sections with a thickness of $4\text{ }\mu\text{m}$. The sections were stained via hematoxylin & eosin (H&E) using standard procedures. Cellular distribution was evaluated via image analysis involving the assessment of nucleus signals. Constructs on the images were equally divided into three sections of upper, center, and bottom regions (Figure 5a). The cell number in each region was counted and divided by the total cell number on the sample to determine cell distribution rates at each region. The cell distribution rate was presented in percentages ($n = 6$).

Preparation of HepG2 Spheroids and Assessment of the Effect of Soluble HGC on Spheroid Fusion. To observe the fusion of spheroids, cells were labeled with DiI or DiO (Vybrant Multicolor Cell-labeling Kit, Invitrogen, CA, USA). Staining was performed according to the manufacturer's instructions. All labeled HepG2 cells (2.5×10^6 cells) were seeded on a 60 mm ULA dish to generate spheroids. After 2 days of culture, all labeled cell aggregates were mixed in one dish, and the media were replaced by a growth medium containing varying concentrations of HGC (0.1, 0.25, or 0.5 wt

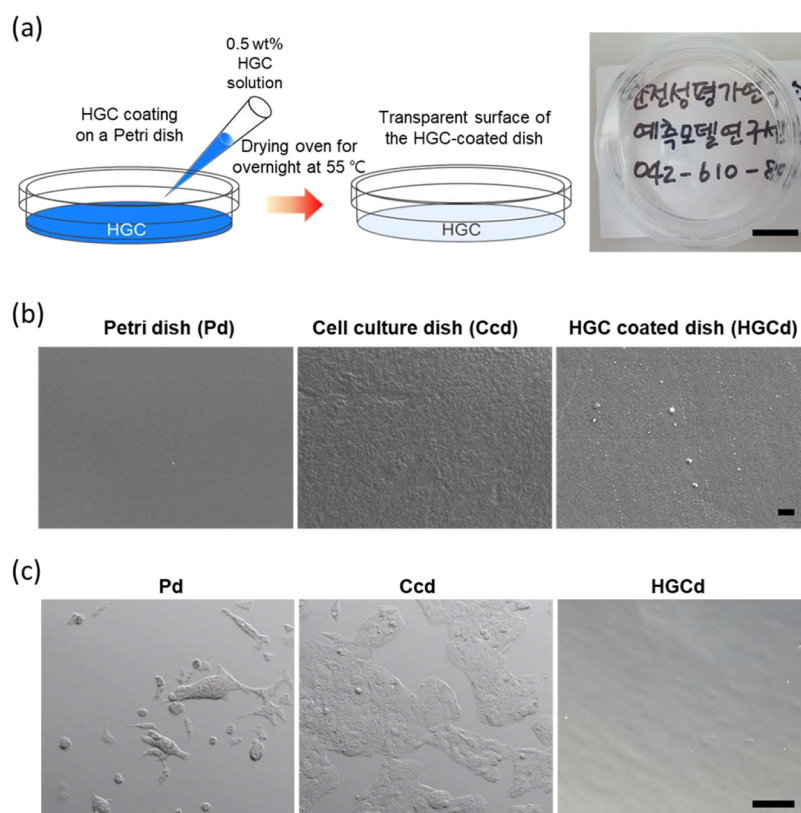


Figure 3. (a) Schematic illustration of HGC coating on a Petri dish and optical image of the HGCd with transparency (scale bar = 1 cm). (b) FE-SEM images of the surface morphologies of a Petri dish (Pd), a cell culture dish (Ccd), and HGCd (scale bar = 1 μm). The images were obtained in the same magnification. (c) Phase-contrast images of HepG2 cells cultured the various substrates for 5 days (scale bar = 100 μm). The images were obtained in the same magnification.

%). Phase-contrast images were obtained during 14 days of culture. The diameter of the spheroids was measured at specific intervals. The obtained values were plotted as histograms according to the HGC concentrations ($n = 300$).

Statistical Analysis. All quantitative data are presented as mean \pm standard deviation (SD). Statistical comparisons were conducted by one-way analysis of variance and Tukey's honest significant difference tests. Results were considered significant for p values less than 0.05.

RESULTS AND DISCUSSION

Characterization of Hexanoyl Glycol Chitosan (HGC).

The HGC was synthesized via the *N*-hexanoylation reaction of glycol chitosan (GC) with hexanoic anhydride (Figure 2a). The chemical composition of HGC was confirmed using $^1\text{H-NMR}$ spectra (Figure 2b). A sharp peak appeared at 3.2–4.0 ppm corresponding to the protons of the glucopyranosyl ring at positions 2–8 (H-2 through H-8). The $^1\text{H-NMR}$ spectrum of HGC (red) showed distinct peaks at 2.31, 1.62, 1.32, and 0.89 ppm compared to the spectrum of GC (black) assigned to $-\text{CO}-\text{CH}_2-$, $-\text{CO}-\text{CH}_2-\text{CH}_2-\text{CH}_2-\text{CH}_2-\text{CH}_3$, $-\text{CO}-\text{CH}_2-\text{CH}_2-\text{CH}_2-\text{CH}_2-\text{CH}_3$, and $-\text{CO}-\text{CH}_2-\text{CH}_2-\text{CH}_2-\text{CH}_2-\text{CH}_3$, respectively. ATR-FTIR analysis was also performed to confirm the synthesis of HGC (Figure 2c). The absorption peak observed at 2890 cm^{-1} was associated with the $-\text{CH}_2$ groups. The appearance of the absorption peak at 1596 cm^{-1} was attributed to vibrations of the amino group of GC. The absorption bands at 1655 and 1555 cm^{-1} corresponded to the carbonyl stretching and amide II bending vibrations of HGC, respectively. For HGC, the amino

vibration band at 1596 cm^{-1} disappeared and the amide II band at 1555 cm^{-1} was intensified. The results of $^1\text{H-NMR}$ spectra and ATR-FTIR analysis were similar to previously reported findings, indicating the successful synthesis of HGC with the degree of hexanoylation being 36.5% ($^1\text{H-NMR}$ characterization).¹² The cytotoxicity of HGC against HepG2 cells was then evaluated by treatment of the cells with HGC mixed in a culture medium at various concentrations (0.1 to 1 wt %) (Figure 2d). All conditions of the various HGC concentrations showed a similar increase in relative proliferation over 7 days of culture. As a result, media supplemented with various concentrations of HGC did not adversely affect the viability of HepG2 cells.

Characterization of HGC-Coated Dishes (HGCd). A Petri dish was subjected to a procedure involving a simple wet coating of HGC (0.5 wt %), as shown in Figure 3a. The coated HGCd did not exhibit crystallization and retained the Petri dish's transparency. Some coating materials employed for surface modification result in opaque surfaces that limit experimental observations. For instance, a material composed of poly-2-hydroxyethyl methacrylate, which is a representative cell repellent material, has low water solubility, resulting in poor visibility due to crystallization.¹⁴

To investigate the effect of HGC coating on morphological changes, the surfaces of Petri dishes (Pd), cell culture dishes (Ccd), and HGC-coated culture dishes (HGCd) were observed via FE-SEM (Figure 3b). Ccd showed a rough surface morphology compared to other groups. HGCd showed a droplet shape; however, most HGC-coated surfaces showed a smooth morphology, similar to that of Pd. The marginal

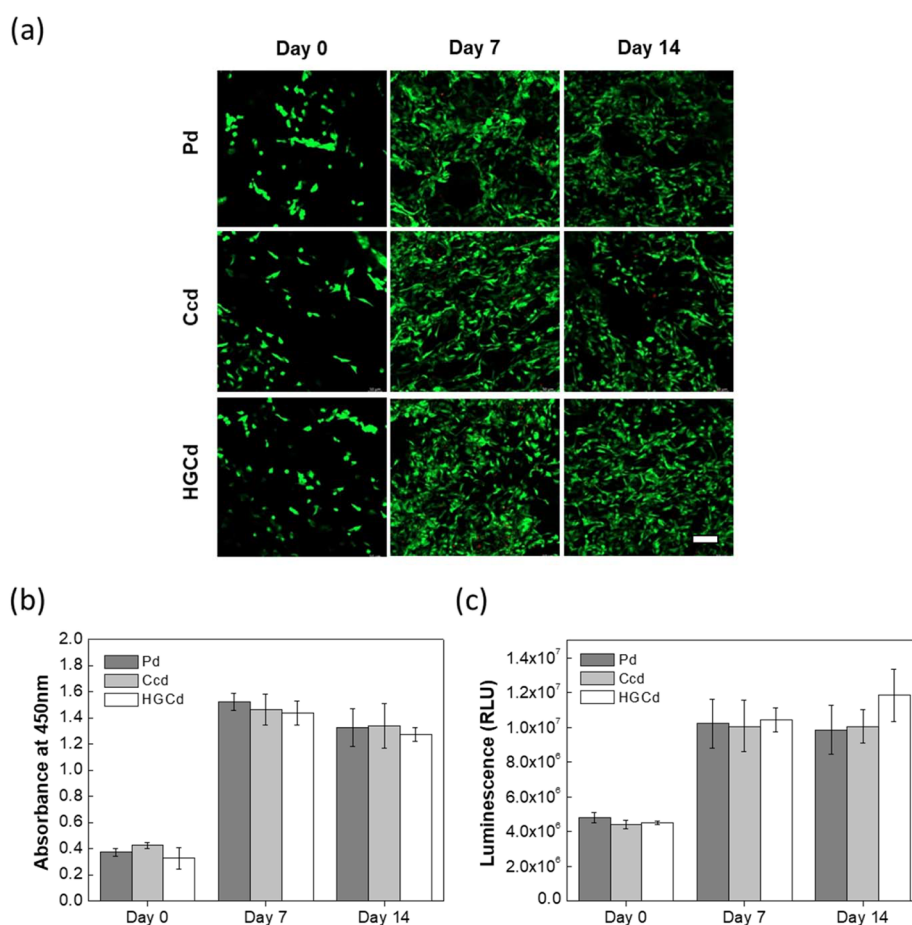


Figure 4. (a) Live/dead staining of HepG2 cells within the constructs at various intervals (scale bar = 100 μm). The images were obtained in the same magnification. (b) CCK-8 cell viability assay and (c) ATP assay of HepG2 cells within the 3D constructs upon the varied substrates.

difference observed in the surface morphology between conditions before and after coating with HGC was similar to that observed in our previous study.¹² Surface roughness is an important parameter for determining cell adhesion and function.¹⁵ Roughness not only increases the surface area but also affects the actin filaments that allow cells to perceive the topology of the surface.¹⁶ The characteristic of the HGC coating, which preserved the original morphology of the target substrate, did not demonstrate unexpected changes in cellular function related to the environmental topology. Then, HepG2 cells were cultured on Pd, Ccd, and HGcd surfaces to evaluate the effect of the surfaces on cell adhesion (Figure 3c). Cells adhered and spread on Pd and Ccd after 3 days following seeding of HepG2 cells. In contrast, cells on HGcd did not show any adhesion. The results show that the surface properties are switched from adhesive to repellent with respect to cells upon coating with HGC without disturbing visibility. To understand how the HGC coating interferes with cell adhesion, water contact angle measurements were performed (Figure S1). The HGC coating converted the surface properties of the Petri dish to hydrophilic. FBS constituting the cell culture medium contains cell adhesive proteins. Proteins are more likely adsorbed to hydrophobic surfaces, and cell adhesive proteins adsorbed to the Petri dish or cell culture plates promote cell adhesion.¹⁷ However, the hydrophilic surface of the HGC-coated surface would prevent adsorption of cell adhesive proteins and interfere with cell adhesion. Several surface modification methods such as agarose

coating have been introduced to form non-cell adhesive plates.¹⁸ Previous studies also understand the inhibition of protein adsorption as the main principle for generation of non-adhesive surfaces. We demonstrated that our HGC coating also formed a non-cell adhesive surface in an easy way, similar to the widely used techniques. Nevertheless, the mechanism for the prevention of cell adhesion by HGC coating is not fully understood and it should be further investigated.

Culture of HepG2 Cell-Laden 3D Collagen Sponge Constructs on HGcd. A highly porous collagen sponge possessing high compatibility for supporting the growth and function of many cell types was selected as a 3D pre-composited scaffold for HepG2 cell culture.¹⁹

The prepared 3D constructs were cultured on supportive substrates of Pd, Ccd, and HGcd. All groups demonstrated good viability by presenting dominant live-cell signals (green) over dead-cell signals (red) regardless of the supportive substrates and intervals (day 0, 7, and 14) (Figure 4a). We then examined proliferation depending on the substrates via the CCK-8 assay (Figure 4b). The constructs exhibited increases in signals on day 7 as compared to day 0 regardless of the groups. The results on day 14 were similar to those on day 7. The ATP assay results also showed a trend very similar to that of the CCK-8 assay results (Figure 4c). We hypothesize that the cells proliferated through the empty space of the collagen sponges during culture and then reached a plateau around day 7 owing to the absence of space for cells to grow inside the collagen sponge. Accordingly, cells functioned

normally during the culture period, but an increase in the value of the proliferation assays would not be observed between days 7 and 14.

We then performed H&E staining with cross sections of the constructs to assess the effect of supportive substrates on cell distribution. Cell distribution was then further analyzed by counting the nuclei in the cross-sectional images divided into upper, middle, and bottom sections (Figure 5). On day 14, in

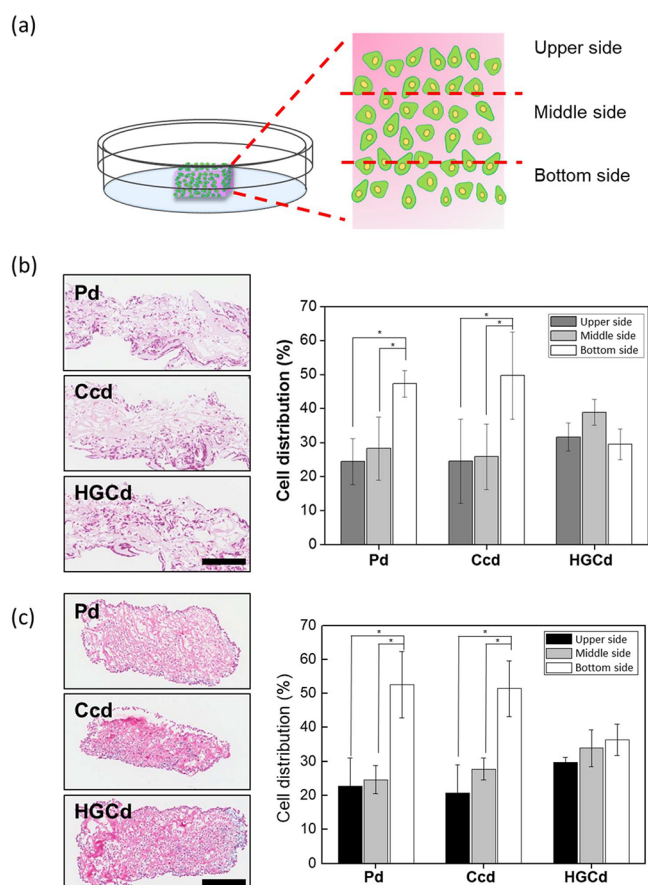


Figure 5. (a) Schematic diagram of sample analysis. (b) H&E staining images captured on day 14 showing the nucleus of HepG2 cells and calculated cell distributions (scale bar = 200 μ m). The images were obtained in the same magnification. “*” indicates statistical significance ($p < 0.05$). (c) H&E staining images on week 4 showing the nucleus of chondrocytes and calculated cell distributions (scale bar = 200 μ m). The images were obtained in the same magnification. “*” indicates statistical significance ($p < 0.05$).

Pd and Ccd groups, approximately 50% of the nuclei were observed on the bottom side, and the rest of the cells were observed on the upper and middle sides, confirming a heterogeneous distribution of cells after the culture (Figure 5b). In contrast, the nuclei were homogeneously distributed throughout the construct in the HGCd group after 14 days of culture. Image analysis also showed 30–40% cell distributions in all regions, confirming a homogeneous cell distribution in 3D constructs of the HGCd group. A similar trend was observed in the culture of the 3D constructs seeded with chondrocytes. Only the chondrocyte-laden 3D constructs cultured on HGCd showed a homogeneous cell distribution after 4 weeks of culture (Figure 5c). Because the cell–cell interactions that determine cell function depend on cell density, maintaining a uniform cell distribution within the

scaffold-based 3D structure is an important feature for the development of functionally reliable products.²⁰ HGCd blocked uncontrolled and ectopic cell migration on the supportive substrate, allowing the cells to maintain a homogeneous distribution within the 3D construct during the culture period. Collectively, HGCd-mediated improvement of cell distribution can overcome the limitations of conventional scaffold-based 3D culture systems in maintaining function and reproducibility.

Effect of HGC Treatment on the Culture of HepG2 Spheroids.

We then introduced HGC into a 3D scaffold-free spheroid culture system. HepG2 spheroids are considered a crucial study model since they demonstrate properties and functions that recapitulate those of the native human liver.²¹ In addition to HepG2 cells, the growing interest in setting up 3D tissue models has prompted the employment of various cellular sources for conventional spheroid formation techniques utilizing ULA with or without micropatterns, microfluidics, hanging methods, magnetic levitation, etc.²² Although these attempts have yielded notable results for the high-throughput generation of spheroids with uniform size and function, technical drawbacks such as uncontrolled fusion between spheroids still remain unresolved.⁹ The provision of soluble HGC in the culture medium is expected to prevent fusion problems via obstruction of the adhesion property of cells composing spheroids. We investigated the effect of various concentrations (0.1, 0.25, and 0.5 wt %) of HGC on spheroid fusion for HepG2 spheroids. In phase-contrast images of the spheroids at day 2 (Figure 6a), all groups showed individually separated spheroids of similar size. On day 5, the control and 0.1 wt % HGC-treated groups demonstrated some spheroids merged with non-spherical structures, while the other two groups still demonstrated individually suspended spheroids. Regardless of the HGC concentrations, the spheroids seemed to grow larger. Many assemblies demonstrated loss of spherical structure and uncontrolled fusion over 7 to 14 days in control and 0.1 and 0.25 wt % HGC-treated groups. In contrast, 0.5 wt % HGC-treated groups maintained individual spheroids for 14 days of culture, presenting a steady increase in size. To quantitatively assess the phenomenon, histograms of the spheroid sizes of each group and time points were plotted (Figure 6b). In the control and 0.1 wt % HGC-treated groups, not only the size distribution at each time point was wide but it was also difficult to find a dominant peak of a specific size in the entire range except on day 2. In contrast, the other groups (0.25 and 0.5 wt % HGC) exhibited relatively narrow size distributions over 14 days of culture. Independently existing spheroids on those groups showed a spontaneous size increase over time, and the arrows indicated at the size showing the highest distribution at each time point shifted to the right as the incubation time increased. The results imply that treatment with 0.5 wt % HGC helped the maintenance of individual spheroids by obstructing fusion via the inhibition of adhesion properties of cells composing spheroids.

Further investigation of the inhibitory effect of HGC on spheroid fusion was conducted by visualizing fluorescent dye-labeled spheroids on ULA-based culture (Figure 7a). Prior to the assembly of spheroids, HepG2 cells were labeled with DIO (green) and DID (red) dyes on TCP. The labeled HepG2 cells were separately cultured on ULA for 2 days. Subsequently, the pre-assembled spheroids were collected and co-cultured until day 14 with varied concentrations of HGC ranging from 0 to 0.5 wt %.

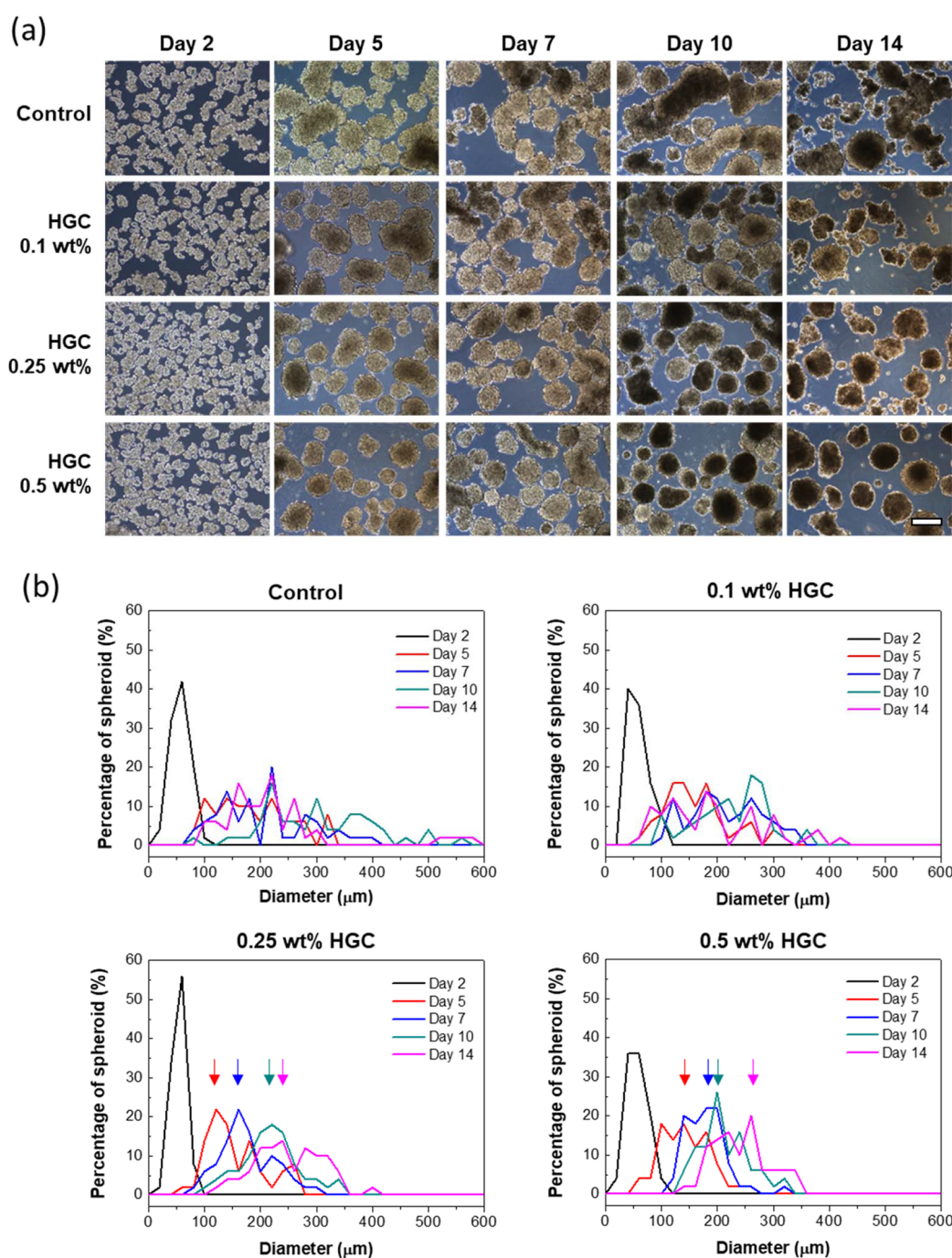


Figure 6. (a) Optical images of the spheroid morphology of HepG2 cells in HGC-containing media (scale bar = 250 μm). The images were obtained in the same magnification. (b) Histogram of spheroid size depending on varying HGC concentrations.

On day 2, all groups showed separate green and red signals. However, spheroids showing both green and red signals were detected in the control group from day 5, indicating induction of spheroid fusion attributed to the innate adhesive property of cells. In contrast, the group supplemented with 0.5 wt % HGC rarely demonstrated spheroids containing both colors in 14 days of culture, evidencing the inhibitory effect of HGC on spheroid fusion. The uncontrollable fusion of spheroids on ULA is of concern not only with respect to functionality and reliability but also for viability associated with the generation of hypoxic conditions.²³ The viability of spheroid culture treated with varying concentrations of HGC for 14 days was examined via live/dead staining (Figure 7b). All groups showed

dominant live-cell signals throughout the structure of the spheroids. However, dead cells were observed at the center of a vigorously merged assembly in the control group as indicated with white dot circles, which could be attributed to hypoxic conditions. Spheroid numbers per well were counted with varied HGC concentrations over 14 days of culture (Figure 7c). Control groups demonstrated a stiff decrease as well as the lowest number on days 7, 10, and 14 as compared to the other groups due to uncontrolled fusion. As the amount of HGC was enhanced, an increase in the spheroid number was observed on days 5, 7, 10, and 14, which aligned with the tendency of the maintenance of individually separated spheroids observed in Figure 5. The generation of spheroids on ULA is known to be

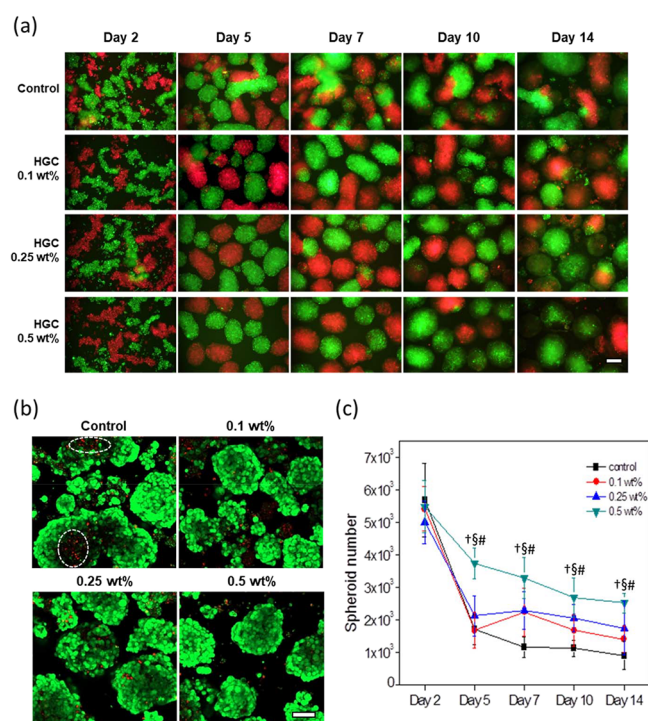


Figure 7. (a) Visualization of spheroid fusion corresponding to varying HGC concentrations (scale bar = 200 μm). The images were obtained in the same magnification. (b) Live/dead assay of the obtained spheroids after 14 days of culture (scale bar = 100 μm). The images were obtained in the same magnification. (c) Count of spheroid numbers per well. “†”, “§”, and “#” indicate statistical significance compared to groups of control and 0.1 and 0.25 wt % HGC, respectively ($p < 0.05$).

initiated upon contact with neighboring cells.²⁴ As cells gather around, cell–cell interactions, dominantly relying on junction proteins, lead to cellular assembly.²⁵ The condensed cell assembly subsequently organizes the spherical structure, while cells at the periphery secrete ECM molecules.⁹ The ECM molecules not only provide an environment suitable for the migration and proliferation of the cells but also function as binding moieties for cells of other neighboring spheroids.²⁶ Various methods such as rotating bioreactor culture and magnetic suspension culture have been introduced to prevent spheroid fusion and to independently culture spheroids for a long time.²⁷ However, an ideal solution for uncontrollable fusion of spheroids has not yet been reported. Although spheroids in the control group were fused, the treatment of the soluble HGC improved the 3D scaffold-free culture, maintaining individual spheroids during 14 days of culture by inhibiting the adhesive property of cells as we hypothesized. Collectively, this study elucidates practical improvements in both the scaffold-based and scaffold-free 3D cultures by exploiting HGC, which might remarkably impact the modeling of artificial tissues for regeneration of damaged tissues, exploring unsolved biological questions, and evaluating next-generation biotherapeutics.

CONCLUSIONS

In this study, we demonstrated remarkable improvements in conventional scaffold-based and scaffold-free 3D cultures by introducing hexanoyl glycol chitosan (HGC), which inhibited the adhesion property of cells. Coating with HGC demon-

strated a surface that prevented cell adhesion, thereby achieving homogeneous cell distribution that ensured the function and reproducibility of scaffold-based 3D culture. Supplementation with HGC during scaffold-free 3D spheroid culture may lead to the mass production of 3D tissue models by preventing contact-mediated fusion. Collectively, the use of HGC will be a universal tool in both scaffold-based and scaffold-free 3D culture systems for the restoration of damaged tissues and preclinical testing as alternatives of animal models for next-generation bioproducts.

ASSOCIATED CONTENT

Supporting Information

The Supporting Information is available free of charge at <https://pubs.acs.org/doi/10.1021/acsomega.2c00890>.

Method and result of the investigation of hydrophilicity by measure of water contact angles on the HGC coated Petri dishes (PDF)

AUTHOR INFORMATION

Corresponding Authors

Kang Moo Huh – Department of Polymer Science and Engineering, Chungnam National University, Daejeon 34134, Republic of Korea; orcid.org/0000-0002-2406-6659; Phone: +82-42-821-6663; Email: khuh@cnu.ac.kr; Fax: +82-42-610-8190

Sun-Woong Kang – Research Group for Biomimetic Advanced Technology, Korea Institute of Toxicology, Daejeon 34114, Republic of Korea; Human and Environmental Toxicology Program, University of Science and Technology, Daejeon 34114, Republic of Korea; orcid.org/0000-0001-8862-2151; Phone: +82-42-610-8209; Email: swkang@kitox.re.kr; Fax: +82-42-610-8157

Authors

Da-Eun Kim – Research Group for Biomimetic Advanced Technology, Korea Institute of Toxicology, Daejeon 34114, Republic of Korea; Department of Polymer Science and Engineering, Chungnam National University, Daejeon 34134, Republic of Korea

Yu Bin Lee – Department of Advanced Toxicology Research, Korea Institute of Toxicology, Daejeon 34114, Republic of Korea

Hye-Eun Shim – Research Group for Biomimetic Advanced Technology, Korea Institute of Toxicology, Daejeon 34114, Republic of Korea; Department of Polymer Science and Engineering, Chungnam National University, Daejeon 34134, Republic of Korea

Jin Jung Song – Research Group for Biomimetic Advanced Technology, Korea Institute of Toxicology, Daejeon 34114, Republic of Korea; Department of Polymer Science and Engineering, Chungnam National University, Daejeon 34134, Republic of Korea

Ji-Seok Han – Department of Toxicological Evaluation and Research, Korea Institute of Toxicology, Daejeon 34114, Republic of Korea

Kyung-Sik Moon – Department of Advanced Toxicology Research, Korea Institute of Toxicology, Daejeon 34114, Republic of Korea

Complete contact information is available at: <https://pubs.acs.org/doi/10.1021/acsomega.2c00890>

Author Contributions

[#]D.-E.K. and Y.B.L. have equally contributed as the first authors. D.-E.K.: investigation, methodology, and formal analysis; Y.B.L.: data curation and writing of original draft; H.-E.S.: methodology, formal analysis, and writing of rebuttal letter and manuscript revision; J.J.S.: methodology and formal analysis; J.-S.H.: methodology and formal analysis; K.-S.M.: funding acquisition and resources; K.M.H.: supervision, funding acquisition, project administration, and writing, review, & editing; S.-W.K.: supervision, funding acquisition, project administration, and writing, review, & editing. All the authors read and approved the manuscript.

Funding

This work was supported by the Basic Science Research Program (NRF-2020R1A2C2100794) of the National Research Foundation of Korea (NRF) funded by the Korean government. This research was supported by the Korea Institute of Toxicology, Republic of Korea (1711133848 and 1711133839). This research was supported by the Korean Fund for Regenerative Medicine (KFRM) grant funded by the Korea government (the Ministry of Science and ICT, the Ministry of Health & Welfare) (KFRM 22A0105L1-11).

Notes

The authors declare no competing financial interest.

REFERENCES

- (1) Kim, J.; Koo, B. K.; Knoblich, J. A. Human organoids: model systems for human biology and medicine. *Nat. Rev. Mol. Cell Biol.* **2020**, *21*, 571–584.
- (2) Sant, S.; Johnston, P. A. The production of 3D tumor spheroids for cancer drug discovery. *Drug Discov. Today Technol.* **2017**, *23*, 27–36. Antoni, D.; Burckel, H.; Jossset, E.; Noel, G. Three-dimensional cell culture: a breakthrough in vivo. *Int. J. Mol. Sci.* **2015**, *16*, 5517–5527. Sirenko, O.; Mitlo, T.; Hesley, J.; Luke, S.; Owens, W.; Cromwell, E. F. High-content assays for characterizing the viability and morphology of 3D cancer spheroid cultures. *Assay Drug Dev. Technol.* **2015**, *13*, 402–414.
- (3) Huang, S. B.; Chou, D.; Chang, Y. H.; Li, K. C.; Chiu, T. K.; Ventikos, Y.; Wu, M. H. Development of a pneumatically driven active cover lid for multi-well microplates for use in perfusion three-dimensional cell culture. *Sci. Rep.* **2015**, *5*, 18352. Goldbard, S. Bringing primary cells to mainstream drug development and drug testing. *Curr. Opin. Drug Discovery Dev.* **2006**, *9*, 110–116. Ohkura, T.; Ohta, K.; Nagao, T.; Kusumoto, K.; Koeda, A.; Ueda, T.; Jomura, T.; Ikeya, T.; Ozeki, E.; Wada, K.; Naitoh, K.; Inoue, Y.; Takahashi, N.; Iwai, H.; Arakawa, H.; Ogihara, T. Evaluation of Human Hepatocytes Cultured by Three-dimensional Spheroid Systems for Drug Metabolism. *Drug Metab. Pharmacokinet.* **2014**, *29*, 373–378.
- (4) Knight, E.; Przyborski, S. Advances in 3D cell culture technologies enabling tissue-like structures to be created in vitro. *J. Anat.* **2015**, *227*, 746–756. Bäcker, A.; Göppert, B.; Sturm, S.; Abaffy, P.; Sollich, T.; Gruhl, F. J. Impact of adjustable cryogel properties on the performance of prostate cancer cells in 3D. *Springerplus* **2016**, *5*, 902.
- (5) Wu, M.-H. Simple poly(dimethylsiloxane) surface modification to control cell adhesion. *Surf. Interface Anal.* **2009**, *41*, 11–16. Yu, T. T.; Shoichet, M. S. Guided cell adhesion and outgrowth in peptide-modified channels for neural tissue engineering. *Biomaterials* **2005**, *26*, 1507–1514. Kale, S.; Biermann, S.; Edwards, C.; Tarnowski, C.; Morris, M.; Long, M. W. Three-dimensional cellular development is essential for ex vivo formation of human bone. *Nat. Biotechnol.* **2000**, *18*, 954–958.
- (6) Langhans, S. A. Three-Dimensional in Vitro Cell Culture Models in Drug Discovery and Drug Repositioning. *Front. Pharmacol.* **2018**, *9*, 6. Carletti, E.; Motta, A.; Migliaresi, C. Scaffolds for tissue engineering and 3D cell culture. *Methods Mol. Biol.* **2011**, *695*, 17–39.
- (7) Wang, K.; Zhou, C.; Hong, Y.; Zhang, X. A review of protein adsorption on bioceramics. *Interface Focus* **2012**, *2*, 259–277. Lee, W. H.; Loo, C. Y.; Rohanizadeh, R. A review of chemical surface modification of bioceramics: effects on protein adsorption and cellular response. *Colloids Surf., B* **2014**, *122*, 823–834. Kelm, J. M.; Fussenegger, M. Microscale tissue engineering using gravity-enforced cell assembly. *Trends Biotechnol.* **2004**, *22*, 195–202. Lee, E.-j.; Chan, E. W. L.; Luo, W.; Yousaf, M. N. Ligand slope, density and affinity direct cell polarity and migration on molecular gradient surfaces. *RSC Adv.* **2014**, *4*, 31581–31588. Gough, A. H.; Chen, N.; Shun, T. Y.; Lezon, T. R.; Boltz, R. C.; Reese, C. E.; Wagner, J.; Verneti, L. A.; Grandis, J. R.; Lee, A. V.; Stern, A. M.; Schurdak, M. E.; Taylor, D. L. Identifying and quantifying heterogeneity in high content analysis: application of heterogeneity indices to drug discovery. *PLoS One* **2014**, *9*, No. e102678.
- (8) Kelm, J. M.; Timmins, N. E.; Brown, C. J.; Fussenegger, M.; Nielsen, L. K. Method for generation of homogeneous multicellular tumor spheroids applicable to a wide variety of cell types. *Biotechnol. Bioeng.* **2003**, *83*, 173–180. Kelm, J. M.; Ehler, E.; Nielsen, L. K.; Schlatter, S.; Perriard, J.-C.; Fussenegger, M. Design of artificial myocardial microtissues. *Tissue Eng.* **2004**, *10*, 201–214. Furukawa, K. S.; Ushida, T.; Sakai, Y.; Suzuki, M.; Tanaka, J.; Tateishi, T. Formation of human fibroblast aggregates (spheroids) by rotational culture. *Cell Transplant.* **2001**, *10*, 441–445. Santini, M. T.; Rainaldi, G. Three-dimensional spheroid model in tumor biology. *Pathobiology* **1999**, *67*, 148–157. Napolitano, A. P.; Dean, D. M.; Man, A. J.; Youssef, J.; Ho, D. N.; Rago, A. P.; Lech, M. P.; Morgan, J. R. Scaffold-free three-dimensional cell culture utilizing micromolded nonadhesive hydrogels. *BioTechniques* **2007**, *43*, 494–500. Pompe, T.; Kaufmann, M.; Kasimir, M.; Johnse, S.; Glorius, S.; Renner, L.; Bobeth, M.; Pompe, W.; Werner, C. Friction-controlled traction force in cell adhesion. *Biophys. J.* **2011**, *101*, 1863–1870. Parsons, J. T.; Horwitz, A. R.; Schwartz, M. A. Cell adhesion: integrating cytoskeletal dynamics and cellular tension. *Nat. Rev. Mol. Cell Biol.* **2010**, *11*, 633–643.
- (9) Lee, Y. B.; Kim, E. M.; Byun, H.; Chang, H. K.; Jeong, K.; Aman, Z. M.; Choi, Y. S.; Park, J.; Shin, H. Engineering spheroids potentiating cell-cell and cell-ECM interactions by self-assembly of stem cell microlayer. *Biomaterials* **2018**, *165*, 105–120.
- (10) Jensen, C.; Teng, Y. Is It Time to Start Transitioning From 2D to 3D Cell Culture? *Front. Mol. Biosci.* **2020**, *7*, 33.
- (11) Lin, S. J.; Jee, S. H.; Hsaio, W. C.; Lee, S. J.; Young, T. H. Formation of melanocyte spheroids on the chitosan-coated surface. *Biomaterials* **2005**, *26*, 1413–1422.
- (12) Cho, M. O.; Li, Z.; Shim, H.-E.; Cho, I.-S.; Nurunnabi, M.; Park, H.; Lee, K. Y.; Moon, S.-H.; Kim, K.-S.; Kang, S.-W.; et al. Bioinspired tuning of glycol chitosan for 3D cell culture. *NPG Asia Mater.* **2016**, *8*, e309–e309.
- (13) Han, S.-S.; Yoon, H. Y.; Yhee, J. Y.; Cho, M. O.; Shim, H.-E.; Jeong, J.-E.; Lee, D.-E.; Kim, K.; Guim, H.; Lee, J. H.; Huh, K. M.; Kang, S. W. In situ cross-linkable hyaluronic acid hydrogels using copper free click chemistry for cartilage tissue engineering. *Polym. Chem.* **2018**, *9*, 20–27.
- (14) Kilic Bektas, C.; Hasirci, V. Cell Loaded GelMA:HEMA IPN hydrogels for corneal stroma engineering. *J. Mater. Sci.: Mater. Med.* **2020**, *31*, 2.
- (15) Giljean, S.; Bigerelle, M.; Anselme, K. Roughness statistical influence on cell adhesion using profilometry and multiscale analysis. *Scanning* **2014**, *36*, 2–10.
- (16) Hou, Y.; Xie, W.; Yu, L.; Camacho, L. C.; Nie, C.; Zhang, M.; Haag, R.; Wei, Q. Surface Roughness Gradients Reveal Topography-Specific Mechanosensitive Responses in Human Mesenchymal Stem Cells. *Small* **2020**, *16*, No. e1905422.
- (17) Lerman, M. J.; Lembong, J.; Muramoto, S.; Gillen, G.; Fisher, J. P. The Evolution of Polystyrene as a Cell Culture Material. *Tissue Eng., Part B* **2018**, *24*, 359–372.
- (18) Lin, X.; Jain, P.; Wu, K.; Hong, D.; Hung, H. C.; O’Kelly, M. B.; Li, B.; Zhang, P.; Yuan, Z.; Jiang, S. Ultralow Fouling and

Functionalizable Surface Chemistry Based on Zwitterionic Carboxybetaine Random Copolymers. *Langmuir* **2019**, *35*, 1544–1551.

(19) Glowacki, J.; Mizuno, S. Collagen scaffolds for tissue engineering. *Biopolymers* **2008**, *89*, 338–344.

(20) Cámara-Torres, M.; Sinha, R.; Mota, C.; Moroni, L. Improving cell distribution on 3D additive manufactured scaffolds through engineered seeding media density and viscosity. *Acta Biomater.* **2020**, *101*, 183–195.

(21) Bokhari, M.; Carnachan, R. J.; Cameron, N. R.; Przyborski, S. A. Culture of HepG2 liver cells on three dimensional polystyrene scaffolds enhances cell structure and function during toxicological challenge. *J Anat* **2007**, *211*, 567–576. Kataoka, K.; Nagao, Y.; Nukui, T.; Akiyama, I.; Tsuru, K.; Hayakawa, S.; Osaka, A.; Huh, N. H. An organic-inorganic hybrid scaffold for the culture of HepG2 cells in a bioreactor. *Biomaterials* **2005**, *26*, 2509–2516.

(22) Ganguli, A.; Mostafa, A.; Saavedra, C.; Kim, Y.; Le, P.; Faramarzi, V.; Feathers, R. W.; Berger, J.; Ramos-Cruz, K. P.; Adeniba, O. et al. Three-dimensional microscale hanging drop arrays with geometric control for drug screening and live tissue imaging. *Sci. Adv.* **2021**, *7* (), DOI: 10.1126/sciadv.abc1323. Lim, W.; Park, S. A Microfluidic Spheroid Culture Device with a Concentration Gradient Generator for High-Throughput Screening of Drug Efficacy. *Molecules* **2018**, *23* (), DOI: 10.3390/molecules23123355. Souza, G. R.; Molina, J. R.; Raphael, R. M.; Ozawa, M. G.; Stark, D. J.; Levin, C. S.; Bronk, L. F.; Ananta, J. S.; Mandelin, J.; Georgescu, M. M.; Bankson, J. A.; Gelovani, J. G.; Killian, T. C.; Arap, W.; Pasqualini, R. Three-dimensional tissue culture based on magnetic cell levitation. *Nat. Nanotechnol.* **2010**, *5*, 291–296.

(23) Schmitz, C.; Potekhina, E.; Belousov, V. V.; Lavrentieva, A. Hypoxia Onset in Mesenchymal Stem Cell Spheroids: Monitoring With Hypoxia Reporter Cells. *Front. Bioeng. Biotechnol.* **2021**, *9*, 611837.

(24) Jakab, K.; Norotte, C.; Damon, B.; Marga, F.; Neagu, A.; Besch-Williford, C. L.; Kachurin, A.; Church, K. H.; Park, H.; Mironov, V.; Markwald, R.; Vunjak-Novakovic, G.; Forgacs, G. Tissue engineering by self-assembly of cells printed into topologically defined structures. *Tissue Eng., Part A* **2008**, *14*, 413–421.

(25) Kang, A.; Seo, H. I.; Chung, B. G.; Lee, S. H. Concave microwell array-mediated three-dimensional tumor model for screening anticancer drug-loaded nanoparticles. *Nanomed.: Nanotechnol., Biol., Med.* **2015**, *11*, 1153–1161.

(26) Frantz, C.; Stewart, K. M.; Weaver, V. M. The extracellular matrix at a glance. *J. Cell Sci.* **2010**, *123*, 4195–4200. (accessed 8/5/2021)

(27) Wu, X.; Su, J.; Wei, J.; Jiang, N.; Ge, X. Recent Advances in Three-Dimensional Stem Cell Culture Systems and Applications. *Stem cells international* **2021**, *2021*, 9477332.